Jpn. J. Appl. Phys. Vol. 38 (1999) pp. 372–375
Part 1, No. 1B, January 1999

Several- and Many-Electron Artificial-Atoms at Filling Factors between 2 and 1

Guy AUSTING[1], Yasuhiro TOKURA[1], Takashi HONDA[1], Seigo TARUCHA[1,3], Martin DANOESASTRO[2], Jorg JANSSEN[2], Tjerk OOSTERKAMP[2] and Leo KOUWENHOVEN[2]

[1]*NTT Basic Research Laboratories, 3-1 Wakamiya, Morinosato, Atsugi, Kanagawa 243-0198, Japan*
[2]*Department of Applied Physics, Delft University of Technology, PO Box 5046, 2600 GA Delft, The Netherlands*
[3]*Department of Physics, University of Tokyo, 7-3-1 Hongo, Bunkyo-ku, Tokyo 113-0033, Japan*

(Received June 1, 1998; accepted for publication September 11, 1998)

We introduce new phenomena that can be studied in an artificial-atom vertical single electron transistor. As we move from the few-electron regime to the several-electron regime, and then the many-electron regime, features in the conductance peaks related to magnetic field induced spin polarization evolve. This allows us to probe the spin-flip region bounded by the last single-particle crossing at low field, and the eventual formation of a maximum density droplet at high field.

KEYWORDS: single electron transistor, double barrier resonant tunneling structure, quantum dot, quantum Hall effect, maximum density droplet, Coulomb blockade, artificial-atom

1. Introduction

Single electron phenomena in single electron transistors continue to attract much attention.[1)] We have reported atomic-like properties of disk-shaped vertical quantum dots fabricated from a GaAs/AlGaAs/InGaAs heterostructure.[2,3)] For an arbitrarily small voltage applied across the dot, V_{sd}, the ground states can be probed directly by measuring the current flowing through the dot as a function of voltage, V_g, applied to a single Schottky gate. Applying a finite V_{sd} and measuring current stripes instead of current peaks, we can also access the first few excited states.

To date we have concentrated on the properties of the ground states when the number of electrons trapped in the dot, N, is between 0 and 20 for a relatively weak magnetic (B-) field up to 3.5 T,[2)] and the properties of ground and excited states in the few-electron regime (N between 0 and 5) for B-fields up to 16 T.[3)] The former is well accounted for by a single-particle picture with a modified constant interaction, and the latter can be understood in terms of many-body effects. The dot is 120 Å thick, and has an effective lateral diameter of about 100 nm in the few-electron limit. The bare lateral confinement energy at 0 T is about 5 meV, and this corresponds to an equivalent cyclotron energy at 2.8 T.[3)]

We now start to expand our study to probe the origin of a number of features in the ground states, which show up strikingly in a B-N phase diagram, as we move out of the few-electron regime. For $N > 5$ we can expect to enter first the several-electron regime, and then eventually the many-electron regime ($N \gtrsim 20$) . Because of the reduction of lateral quantization and increased electron screening as N increases, a two-dimensional (2D) limit is approached for large N. Particularly in the presence of a B-field, which strengthens electron interactions, we would expect to see features that can be related to those familiar in the Quantum Hall effect. In particular, the concept of a filling factor, ν, becomes very useful.

In this paper we make a simple connection between different regions of the B-N phase diagram. Features which can be fully explained by exact-diagonalization techniques incorporating many-body effects up to $N = 5$ in the few-electron regime[3–5)] evolve into features in the several- and many-electron regimes (not amenable to exact-diagonalization) which reflect a larger dot with a more 2D character. In particular, as the B-field is increased beyond that required to achieve $\nu = 2$, from 'cusps' and 'steps' in the position of the conductance peaks, we identify a spin-flip regime, before the formation of a maximum density droplet (MDD) at $\nu = 1$.

For planar-dot devices containing many-electrons ($N \approx 40$), a classical self-consistent model has been introduced to account for features in the $2 > \nu > 1$ region.[6,7)] Self-consistent charge distribution in the dot results in the compressible center (second Landau level partially occupied) being separated from the compressible edge (lowest Landau level partially occupied) by an incompressible 'ring' in which the lowest Landau level is completely filled. Sequential depopulation occurs as electrons transfer across the 'ring' from spin-down sites in the second Landau level at the center to spin-up sites in the lowest Landau level at the edge. This gives rise to $N/2$ 'wiggles' in the conductance peaks which are usually well resolved.[1,6,7)] It is worth stressing that because of the geometry of a planar-dot, edge states in the emitter are well resolved, so the current is carried principally by the strong coupling of these states to nearby edge states in the dot. In an increasing B-field, the chemical potential at the dot center and dot edge is respectively raised and lowered. Eventually it is energetically favourable for an electron to transfer from a spin-down site at the center to a spin-up site at the edge, so a spin-flip is accompanied by an increase in the chemical-potential at the dot edge. As the conductance peak is effectively a measure of the chemical-potential of the edge of the planar-dot, the conductance peak 'jumps-up'. A sequence of $N/2$ spin-flips gives rise to 'saw-tooth'-like oscillations in the peak position.

Until now only two terminal capacitance-voltage measurements of a vertical quantum dot have permitted access to the Quantum Hall region in a many-electron artificial atom.[8,9)] Between $2 > \nu > 1$ for $N \approx 40$ a sequence of 'bumps' is observed, but the 'bumps' are quite hard to see, and their number is much less than $N/2$.

2. Device and Experimental Details

Full details of the material parameters and device fabrication are described elsewhere.[10)] The starting material is a specially designed double barrier resonant tunneling structure with an $In_{0.05}Ga_{0.95}As$ well, $Al_{0.22}Ga_{0.78}As$ barriers, and n-doped GaAs contacts.[2)] This material is processed to form circular mesas by a special etching technique.[11)] In this paper

we discuss two devices A and B which both have a geometrical diameter of 0.54 μm. Measurements on device A and B are performed in a dilution refrigerator and in a ^{3}He cryostat respectively. The B-field is applied parallel to the tunneling current.

3. Discussion

Figure 1 shows the B-N phase diagram for device A for N from 0 to about 14. V_{sd} is $\approx$100 μV, so the positions of the conductance peaks obtained by sweeping V_g from about -2.1 V to -1.0 V reflect the ground states, and these evolve in an intricate manner as the B-field is changed from 0 T to 7 T. We now describe and classify the various features and regions.

At 0 T, a shell structure is observed in the addition energy, and Hund's rule is obeyed.[2] In Fig. 1 large peak spacings for $N = 2$, 6, and 12 (the first three magic numbers for a 2D harmonic potential) identify the completion of the first three shells. The relatively large peak spacing for $N = 4$ ('H') is a consequence of an exchange effect when the two degenerate levels in the second shell are half filled.

When the B-field is first applied, we see a general pairing of peaks due to spin-degeneracy, and 'wiggles' due to crossings of single-particle states.[2] For $N > 4$, the last 'wiggle' occurs when the single-particle states last cross. Beyond the last 'wiggle' these states merge to form Landau levels. The last 'wiggle' for $N = 5$ is marked by a diamond in Fig. 1. We can follow this last 'wiggle' for higher N. B-fields at which the last 'wiggle' occurs can be identified with $\nu = 2$. This means that for even N, the ground state is spin-unpolarized (the total spin, S, is 0), and the total angular momentum, M, is $N(N-2)/4$.

In the absence of Coulomb interactions, there would be no other transitions in the ground states beyond that required to achieve $\nu = 2$ if the weak Zeeman effect is neglected. However, in the presence of many-body effects, B-field induced transitions in the N-electron ground states occur in such a way that M is increased, and S is maximized. The former is favoured by the direct Coulomb energy and influenced by the kinetic energy, while the latter is favoured by exchange and Zeeman energies, and modified by correlation effects.[4,5,12–15]

For $N < 6$ we have measured current peaks and stripes to track B-field induced transitions beyond $\nu = 2$.[3] Our spectra compare well with those calculated by exact-diagonalization incorporating many-body effects. This has allowed us to identify the quantum numbers of the electronic configurations of the ground and first few excited states.[3–5] In Fig. 1 the black triangle locates the position of the singlet-triplet transition for $N = 2$. In a single spin-flip, the 2-electron system has become completely spin-polarized. For $N > 2$ the process of spin-polarization occurs over a finite B-field range. Weak 'cusps' marked by open and black circles respectively mark where this process begins and ends. At B-fields marked by the black triangle and black circles the N-electron system has become completely spin-polarized. S is $N/2$ and M is $N(N-1)/2$. Between the open and the black circles: 1. not all the predicted transitions can be readily observed (particularly true for $N > 3$) as they can occur very close to one another, i.e. ground and excited states are very close in energy,[16] 2. not all transitions actually involve a spin-flip (some just involve a change to higher M, although one would expect for even N and odd N respectively, $N/2$ and $(N-1)/2$ spin-flips),[16] and 3. for a given S and M, more than one configuration of single-particle states can be important.[3]

Figure 2 shows the B-N phase diagram for device B for N from 5 to about 10. There seem to be one or two weak 'cusp'-like features (marked by arrows) before the final feature at $\approx$6 T which is identified with $\nu = 1$. The number of features does not clearly increase directly with N, so it seems that not all the expected transitions for $2 > \nu > 1$ can be distinguished. Although we have just entered the several-electron

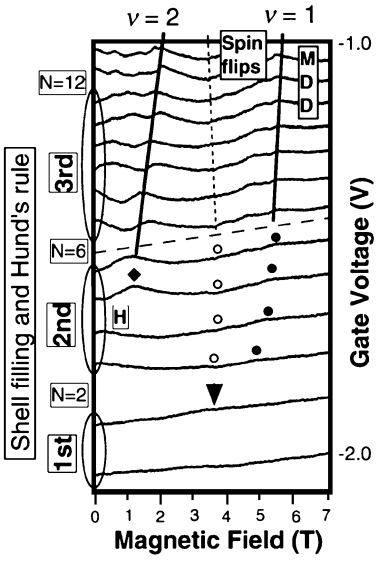

Fig. 1. B-N phase diagram for device A covering N from 0 to about 14 measured in a dilution refrigerator. V_{sd} is $\approx$100 μV, V_g is varied from about -2.1 V to -1.0 V, and the B-field is swept from 0 T to 7 T. The positions of the conductance peaks evolve in an intricate manner. Various regions can be identified. The symbols are discussed in the text.

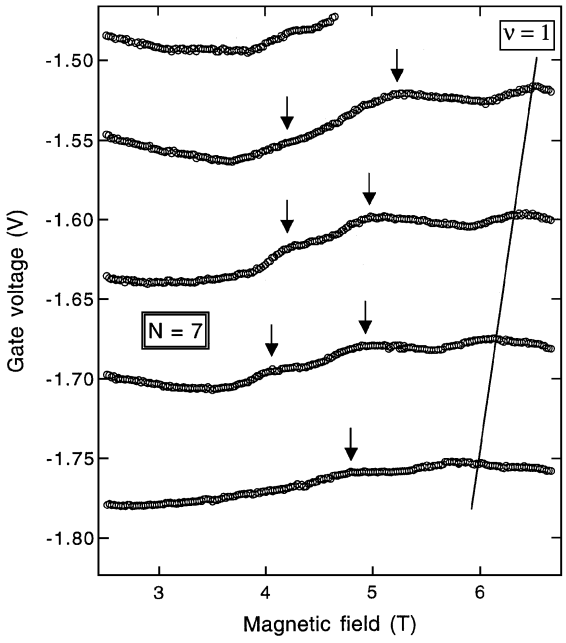

Fig. 2. B-N phase diagram for device B covering N from 5 to about 10 measured in a ^{3}He cryostat. V_{sd} is $\approx$40 μV, V_g is varied from about -1.8 V to -1.5 V, and the B-field is from 2.5 T to 6.7 T. Arrows mark weak 'cusps'.

regime, it is currently not amenable to exact-diagonalization techniques. Crucially, N is not sufficiently large that we can meaningfully define compressible and incompressible regions in the dot, and the MDD phase too is not really fixed for $\nu < 1$. The many-body ground and excited states are still expected to be important, and B-field induced transitions are presumably responsible for the weak 'cusps', although we can not label the states at present

As we increase N well into the several-electron regime (reducing the confinement still further), there will come a point when N is sufficiently large that the model of McEuen *et al.* may be helpful.[6,7] Figure 3 shows the B-N phase diagram for device B in the region of $N \approx 25$. From ≈0.8 T beyond $\nu = 2$ there is a sequence of six or seven features (marked by thick bars) before the final feature at ≈6.2 T ($\nu = 1$ and the start of the MDD). Compared with Fig. 2, the shape of the features in Fig. 3 is now very different, and they change in form from 'cusp'-like at low field to 'step'-like and even 'peak'-like at high field. Although more numerous than in Fig. 2, the number of features again does not really increase with N for consecutive conductance peaks. Compressible and incompressible regions within the dot have now formed, and the MDD phase for $\nu < 1$ is much clearer, but still we can expect a small but finite excitation energy in the single particle picture. Many-body ground and excited states are probably still important, and the broad 'peak' just beyond 5 T may be a remnant of the right most arrow in Fig. 2.

Finally, we move into the many-electron regime and yet weaker confinement. Figure 4 shows the B-N phase diagram for device B in the region of $N \approx 45$ which is comparable in N to the dot-systems described by McEuen *et al.*[6,7] and Ashoori.[9] From ≈0.5 T beyond $\nu = 2$ there is now a string of about nine or ten features (marked by ovals) before the last feature at ≈6.2 T ($\nu = 1$ and the start of the MDD). The appearance of the features in Fig. 4 is similar to that in Fig. 3 (but perhaps a little more distinct), changing from 'cusp'-like at low field to 'step'-like and 'peak'-like at high field. Yet again the number of features does not really increase with N for successive conductance peaks, and the number is certainly a lot less than $N/2$. Note that the capacitance-voltage data of Ashoori only reveals one or two clear features before $\nu = 1$.[9] We now expect compressible and incompressible regions inside the dot and the MDD phase to be very well established. Many-body states are now not expected to be important, and this may explain why the broad 'peak' just beyond 5 T in Fig. 3 is no longer clear in Fig. 4. Naively, the simple picture of McEuen *et al.* should be applicable, and yet for our vertical-dot the appearance of the spin-flips overall, and their number is very different from that in the planar-dots.[6,7,20]

Based on our observations, and those of Ashoori,[9] it seems that the spin-flip characteristics in a vertical-dot are different to those in a planar-dot, i.e. geometry is important. The influence of the emitter in the former is not well understood. We can see in Figs. 3 and 4 that between 3 and 5 T the features are more 'cusp'-like, whereas from 5 T to $\nu = 1$ they are more 'step'-like or 'peak'-like. It is probable that at lower field there are incomplete edge states in the emitter, so the complex nature of these states and how they couple to dot states across the emitter barrier could strongly influence the spin-flip features. At higher field, just before $\nu = 1$, edge states in the emitter may be better defined so the appearance

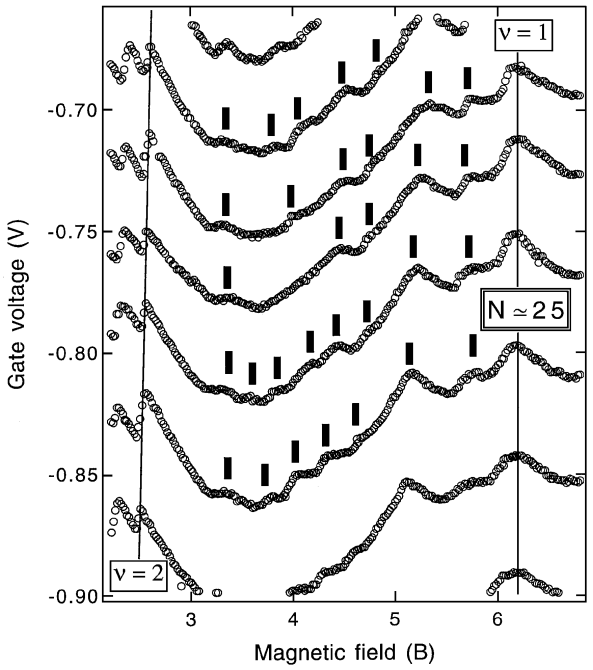

Fig. 3. B-N phase diagram for device B in the region of $N \approx 25$ measured in a ^{3}He cryostat. V_{sd} is ≈30 μV, V_g is varied from about −0.9 V to −0.65 V, and the B-field is from 2.2 T to 6.8 T. Thick bars mark identifiable features over five consecutive peaks.

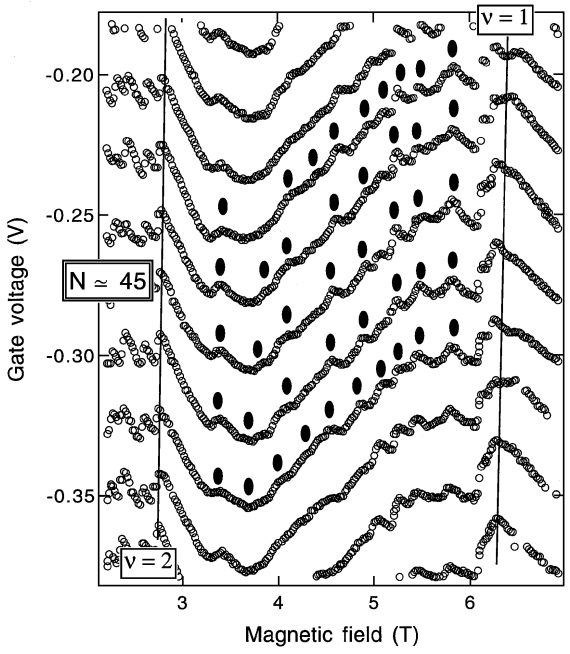

Fig. 4. B-N phase diagram for device B in the region of $N \approx 45$ measured in a ^{3}He cryostat. V_{sd} is ≈30 μV, V_g is varied from about −0.35 V to −0.2 V, and the B-field is from 2.2 T to 6.95 T. Ovals mark identifiable features over five consecutive peaks.

of the spin-flips might change. In short, it is not clear what the conductance peak is tracking, although the features we see at high N just before $\nu = 1$ are closer in appearance to the spin-flips reported for planar-dots.[6,7] These issues deserve further investigation.

In subsequent work on planar-dots by Klein *et al.*, the self-consistent model was superseded by a Hartree-Fock (H-F) model to explain a number of important experimental obser-

vations.[17] Even so, H-F could not account for the very small average level spacing deduced from non-linear conductance traces in the $2 > \nu > 1$ region. While H-F is well suited to the MDD region, it may not be so good in the spin-flip region since there are many close-lying states. For a better understanding of the spin-flip region a density-functional approach, as employed by Stoof and Bauer,[18] may be more appropriate. Figures 3 and 4 give clues about the relative importance of factors contributing to the appearance of the conductance peaks for $2 > \nu > 1$ at large N. At and immediately beyond $\nu = 2$, a weak even-odd asymmetry in N for peak spacings indicates that the single particle excitation energy is not negligibly small. However, $\approx$1 T beyond $\nu = 2$, this asymmetry is less evident, so while the single particle excitation energy has reduced, the Landau levels are better resolved, and direct Coulomb and exchange are becoming more important.

The electron density in the $In_{0.05}Ga_{0.95}As$ well of the starting material is self-consistently calculated to be $1.67 \times 10^{11}\,cm^{-2}$. The density deduced from Shubnikov-de Haas measurements on extremely large diameter ($>50\,\mu$m) devices is about $1.7 \times 10^{11}\,cm^{-2}$ ($\nu = 2$ and $\nu = 1$ occur respectively at 3.5 T and $\approx$7 T).[19] $\nu = 2$ and $\nu = 1$ are located in Fig. 1 respectively at about 2 T and 5.5 T for $N = 14$, These values increase further at larger N (see Figs. 3 and 4). Note that we expect the density in the sub-micron gated mesas to be less than that for very large devices because of the importance of surface depletion effects in the former. For sufficiently large N, an increasing gate voltage increases the area of the dot and N in such a way that the density tends to a constant. This is why, for example, the B-field for the last single-particle crossing changes very little for $N > 20$ (see Figs. 3 and 4).

For completeness, we state again that $\nu = 1$ marks the beginning of a distinct maximum density droplet phase for N larger than about 10 in which all N-electrons are in the lowest Landau level, and all the single-particle states $(n, l) = (0, 0), (0, 1), \ldots, (0, N-1)$ are occupied by one spin-up electron (n and l respectively are the radial and angular momentum quantum numbers for a 2D harmonic potential).[1] The detailed properties of this phase and beyond for $\nu < 1$ will be discussed elsewhere.

4. Conclusion

Well defined artificial semiconductor atoms are ideal for studying the properties of electrons in the Quantum Hall region beyond the few-electron regime, in the several- and many-electron regimes. Features in the position of conductance peaks in the $2 > \nu > 1$ region can be related to magnetic field induced spin polarization. The spin-flip region is bounded by the last single-particle crossing at low field ($\nu = 2$), and the eventual formation of a maximum density droplet at high field ($\nu = 1$). Spin-flip related features change from weak 'cusps' for $6 < N < 12$ to complex 'cusps', 'steps', and 'peaks' for $N > 20$. We hope our experimental observations will stimulate theoretical descriptions of vertical-dots.

1) U. Meirav and E. B. Foxman: Semicond. Sci. Technol. **11** (1996) 255.
2) S. Tarucha, D. G. Austing, T. Honda, R. J. van der Hage and L. P. Kouwenhoven: Phys. Rev. Lett. **77** (1996) 3613.
3) L. P. Kouwenhoven, T. H. Oosterkamp, M. W. S. Danoesastro, M. Eto, D. G. Austing, T. Honda and S. Tarucha: Science **278** (1997) 1788.
4) M. Eto: Jpn. J. Appl. Phys. **36** (1997) 3924.
5) Y. Tokura, L. P. Kouwenhoven, D. G. Austing and S Tarucha: Physica B **246-247** (1998), 83.
6) P. L. McEuen, E. B. Foxman, J. Kinaret, U. Meirav, M. A. Kastner, N. S. Wingreen and S. J. Wind: Phys. Rev. B **45** (1992) 11419.
7) P. L. McEuen, N. S. Wingreen, E. B. Foxman, J. Kinaret, U. Meirav, M. A. Kastner, Y. Meir and S. J. Wind: Physica B **189** (1993) 70.
8) R. C. Ashoori, H. L. Stormer, J. S. Weiner, L. N. Pfeiffer, K. W. Baldwin and K. W. West: Phys. Rev. Lett. **71** (1993) 613.
9) R. C. Ashoori: Nature **379** (1996) 413.
10) D. G. Austing, T. Honda, Y. Tokura and S. Tarucha: Jpn. J. Appl. Phys. **34** (1995) 1320.
11) D. G. Austing, T. Honda and S. Tarucha: Semicond. Sci. Technol. **11** (1996) 388.
12) P. A. Maksym and T. Chakraborty: Phys. Rev. B **45** (1992) 180.
13) M. Wagner, U. Merkt and A. V. Chaplick: Phys. Rev. B **45** (1992) 1951.
14) P. Hawrylak: Phys. Rev. Lett. **71** (1993) 3347.
15) J. J. Palacios, L. Martín-Moreno, G. Chiappe, E. Louis and C. Tejedor: Phys. Rev. B **50** (1994) 5760.
16) S. Tarucha, T. Honda, D. G. Austing, Y. Tokura, K. Muraki, T. H. Oosterkamp, J. W. Janssen and L. P. Kouwenhoven: Physica **E3** (1998) 112.
17) O. Klein, D. Goldhaber-Gordon, C. de C. Chamon and M. A. Kastner: Phys. Rev. B **53** (1995) R4221.
18) T. H. Stoof and G. E. W. Bauer: Solid-State Electron. **40** (1996) 349.
19) K. Muraki: private communication.
20) A. Sachrajda and P. Hawrylak: private communication.